Journal of Alloys and Compounds 519 (2012) 140–143

Contents lists available at SciVerse ScienceDirect

Journal of Alloys and Compounds

journal homepage: www.elsevier.com/locate/jallcom

# Rectifying behavior and transport mechanisms of currents in $Pt/BaTiO_3/Nb:SrTiO_3$ structure

R.K. Pan [a], T.J. Zhang [a,*], J.Z. Wang [a], Z.J. Ma [a], J.Y. Wang [a], D.F. Wang [a,b]

[a] School of Materials Science & Engineering, Hubei University, Wuhan 430062, PR China
[b] q-Psi & Department of Physics, Hanyang University, Seoul 133-791, Republic of Korea

ARTICLE INFO

*Article history:*
Received 25 October 2011
Received in revised form
26 December 2011
Accepted 28 December 2011
Available online 5 January 2012

*Keywords:*
$BaTiO_3$ film
Rectifying
Schottky barrier
Current mechanism

ABSTRACT

The 15-nm-thickness $BaTiO_3$ (BTO) epitaxial film was prepared on the Nb-doped $SrTiO_3$ (NSTO) single crystal substrate using pulsed laser deposition technique. The morphology and structure of the film was measured by the AFM, TEM and XRD, respectively. The current–voltage curves show abnormal backward diode-like rectifying behavior at room temperature, which was discussed using the Schottky barrier model taking into account the movement of oxygen vacancies. The leakage currents under reverse bias were excellently fitted by the Poole–Frenkel (P–F) emission and Fowler–Nordheim (F–N) tunneling mechanisms, respectively. At forward bias, the current was fitted by the space-charge-limited current mechanism. The C–V curves indicate that there is a positive build-in voltage (about 0.56 V) in the Pt/BTO/NSTO structure, which confirms the backward rectifying behavior.



## 1. Introduction

Recently the rectifying properties of many heterojunctions are studied due to their widely applications in various semiconductor devices. Among these junctions, p–n junctions made of oxides are expected to work at a high temperature and cause much attention [1–5]. Reports show that Nb-doped $SrTiO_3$ single crystal behaves like a metal, suggesting that NSTO is a degenerate n-type semiconductor with a band gap of 3.2 eV [6]. Using as both substrate and bottom electrode, NSTO is well lattice matched with $BaTiO_3$, $(Ba_xSr_{1-x})TiO_3$ or $Pb(Zr,Ti)O_3$, which makes it easy to epitaxially grow BTO thin films. The p–n junctions with NSTO used as n-type oxide substrate are also interesting to be investigated [7–11]. Considering the carrier transport at the interface near the p–n junction, the current–voltage ($I$–$V$) rectifying effect was usually described by the exponential relation [12],

$$I = I_s \exp\left(\frac{qV}{\eta kT}\right) \quad (1)$$

where $q$ is the electronic charge, $V$ is the applied voltage, $k$ is the Boltzmann constant, $\eta$ is the ideality factor and $I_s$ is the reverse saturation current of junction.

Cui et al. reported the rectifying properties of $TbMnO_3$/NSTO p–n junctions and investigated the abnormal backward diode-like behaviors at low temperature [6,7]. He suggested the backward diode-like behavior can be originated from the tunneling current through $TbMnO_3$/NSTO p–n junction instead of the thermionic emission [7]. Luo et al. studied $Pr_{0.7}Ca_{0.3}MnO_3$/NSTO junctions and the results showed that the $J$–$V$ characteristics of these heterojunctions can be well-fitted by the thermally assisted tunneling model [9]. Large rectifying currents and resistive hysteresis were also found at the interface between two n-type semiconductors besides the interface of p–n junctions [13]. In this paper, large rectifying currents in the Pt/BTO/NSTO structure were observed at room temperature, which also showed above-mentioned backward diode-like behavior. The leakage currents were excellently fitted by the P–F emission and F–N tunneling mechanisms, respectively, which may have an insight into understanding the abnormal backward rectifying behavior.

## 2. Experimental

The epitaxial BTO film was grown by the pulsed laser deposition technique at 700 °C on the one-side-polished Nb–0.7 wt%-doped $SrTiO_3$ single-crystal substrate, which size is 10 mm × 10 mm. The electrical resistivity of the NSTO substrates is about 7.0 mΩ cm at room temperature, which exhibits metal conductive behavior. The substrates were chemically and thermally treated [14,15]. A KrF excimer laser (248 nm) operating at 2 J/cm$^2$ was focused on the surface of a rotating target at a 45° angle of incidence. The NSTO substrate was placed on a heater, which was 50 mm away from the target. The working pressure during the depositing was maintained at 0.1 Pa by $O_2$ flow rate of 40 sccm. After the deposition, The BTO film was annealed at 750 °C for 1 h in the tube furnace in air. The topography and microstructure of the BTO film were examined by an atomic force microscopy (AFM: DI, Nanoscope II), high-resolution transmission electron microscopy (HRTEM: JEOL, JEM-2100F) and X-ray diffraction (XRD: Bruker, D8 Advance). 100-nm-thick Pt layer patterned by the

* Corresponding author. Tel.: +86 27 88661571; fax: +86 27 88664297.
*E-mail address:* tj65zhang@yahoo.com.cn (T.J. Zhang).

0925-8388/$ – see front matter © 2012 Elsevier B.V. All rights reserved.
doi:10.1016/j.jallcom.2011.12.146

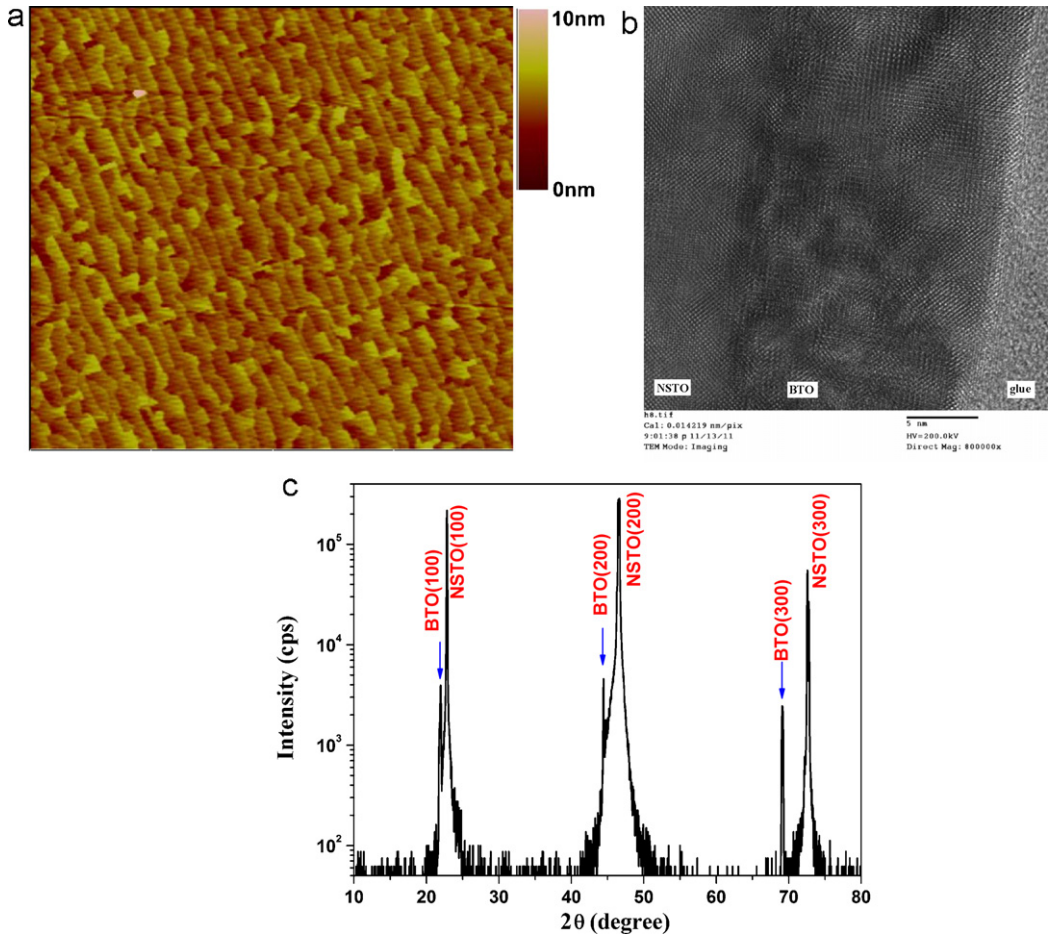


**Fig. 1.** The AFM topography image (1 μm × 1 μm area) (a), HRTEM image (cross-section view) (b), and the XRD pattern (c) of the BTO film grown on the NSTO substrate.

metal mask was deposited as top electrode (diameter = 0.2 mm) using dc magnetic controlled sputtering technique at room temperature. The In film bottom electrode (about 1 $mm^2$) was pressed on the NSTO substrate. The *I–V* measurements were performed at room temperature by an unswitched linear voltage sweep to the top electrode, using a ferroelectric parameter test system (RT, Precision Premier II). A forward bias applied to the BTO film is defined as the current flowing from the top Pt electrode into the BTO film (see the insert in Fig. 2). At each voltage step, the delay time and the measure time are identical (0.1 s). The soak time is 0.2 s.

The C–V curves were measured by a precision impedance analyzer (Agilent 4294A), a small ac signal of 50 mV was employed at 10 kHz, 100 kHz and 1 MHz, respectively. The dc voltage was firstly scanned from −1.5 V to +1.5 V, and then scanned from +1.5 V to −1.5 V with a step of 0.1 V. The leakage currents are so large that only 1.5 V can be applied.

## 3. Results and discussion

The surface quality of the BTO film was characterized by AFM. 1 μm × 1 μm AFM image is presented in Fig. 1(a). The BTO thin film had a smooth and uniform surface. The root mean square (RMS) is 0.82 nm. Fig. 1(b) illustrates a HRTEM lattice image of the BTO/NSTO structure, which displays the epitaxial crystallographic relationship. The thickness of the film is about 15 nm. The XRD pattern in Fig. 1(c) shows clearly the separated peaks, which also indicate that the BTO film grew hetero-epitaxially on the NSTO (1 0 0) substrate.

The *I–V* curves under forward and reverse bias are shown in Fig. 2, which clearly demonstrate a backward diode-like rectifying behavior. The rectification ratio is about 85 (1 0 1) at bias voltage 3 V (4 V).

For the epitaxial BTO film on the NSTO substrate, the barrier height at the interface of BTO/NSTO is low. Because the band gaps are almost same (about 3.2 eV) and the difference between the work functions 4.08 (NSTO) − 3.9 (BTO) ≈ 0.18 eV is small [3,6,16]. The barrier height at Pt/BTO is about 1.7 eV.

Yang et al. reported that the rectifying *I–V* characteristic originates from the $BFeO_3$/Nb-STO p–n junction [3,17]. According to Eq. (1), the forward *I–V* characteristic of a p–n junction can be identified by the linear relation of Ln *I–V* curves. But the nonlinear relation of

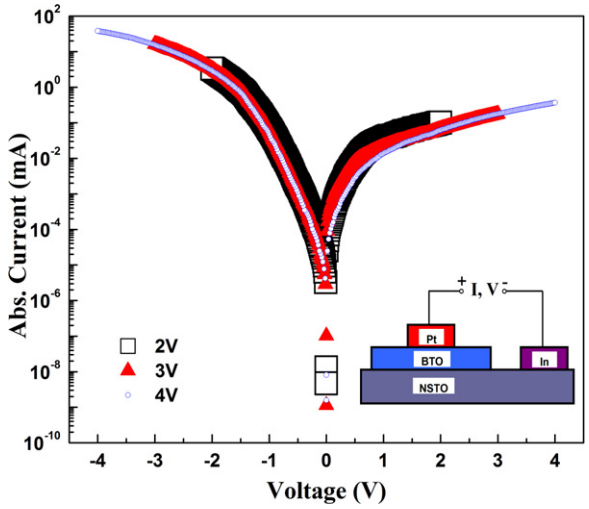


**Fig. 2.** The *I–V* curves in log-log scale for the Pt/BTO/NSTO structure. Maximum voltages are 2 V (open square), 3 V (solid triangular) and 4 V (open circle), respectively. The insert shows the measurement schematic of a conventional sandwiched structure (not to scale).

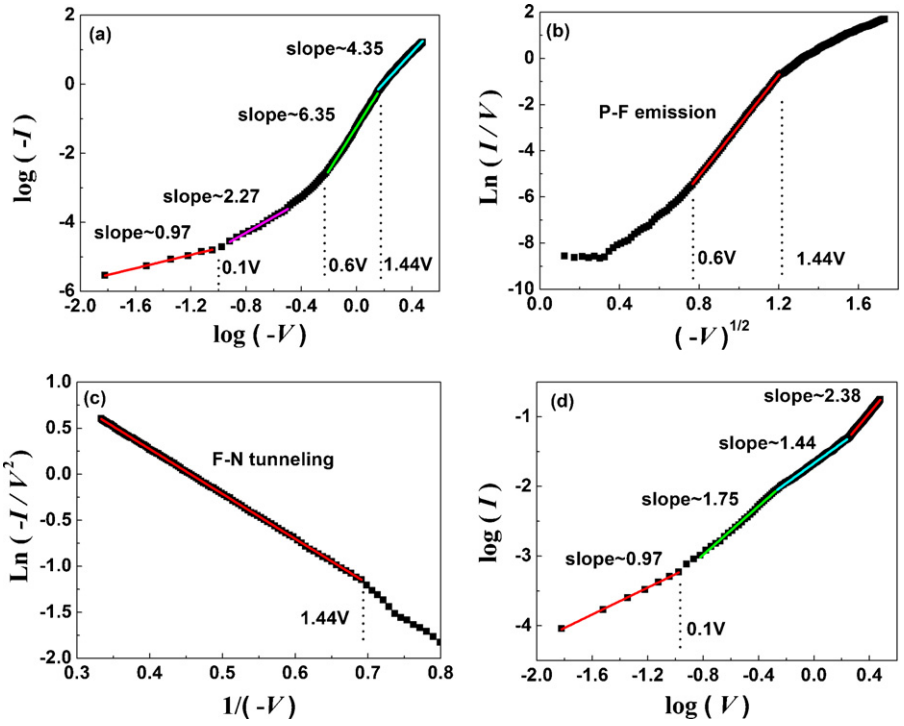


**Fig. 3.** (a) The *I–V* curve in log-log scale under the reverse bias of 3 V. (b) Plots of $\mathrm{Ln}(I/V) \sim (-V)^{1/2}$ show the P–F emission under the reverse bias from 0.6 V to 1.44 V. (c) Plots of $-\mathrm{Ln}(-I/V^2) \sim 1/V$ show the F–N tunneling under the reverse bias exceeds 1.44 V. (d) The *I–V* curve in log-log scale under the forward bias of 3 V.

the Ln *I–V* curve in Fig. 2 indicates that the rectifying behavior of the configuration of Pt/BT/NSTO is dominated by other mechanisms instead of the p–n junction effect.

For nonlinear conduction mechanisms of the Schottky barrier, there are space-charge-limited conduction (SCLC) with a linear relation of $I \propto V^2$, Schottky emission with a linear relation of $\log I \propto V^{1/2}$, Poole–Frenkel emission with a linear relation of $\log(I/V) \propto V^{1/2}$ and Fowler–Nordheim tunneling with $\log(I/V^2) \propto 1/V$ [12,18]. The *I–V* curve of the Pt/BTO/NSTO structure measured at reverse bias of 3 V is drawn in log-log scale in Fig. 3(a). All standard errors of these linear fittings are below 0.02. And the Adj. *R*-Squares are higher than 0.998. We can distinguish the conduction mechanisms according the slopes of the $\log I \sim \log V$ curve. At low reverse bias (<0.1 V), the slope is around unity imply that the ohmic conduction is the dominant leakage mechanism. When the reverse bias increases (0.1–0.6 V), the slope is about 2.27 (close to 2), which indicates SCLC conduction. At higher reverse bias, the slopes become much bigger than 2, which indicate P–F emission and other conduction mechanisms. Fig. 3(b) and (c) shows that the *I–V* curve can be excellently fitted by P–F emission at −0.6 V to −1.44 V bias and F–N tunneling exceeding about −1.44 V, respectively.

Safari et al. mentioned that the P–F coefficient $\beta_{PF}$ can distinguish P–F emission from other mechanisms by calculating the slope of the fitted line $\beta_{PF}/k_BT$ [19],

$$J = \sigma_0 E \exp\left(\frac{\beta_{PF}E^{0.5} - \Phi_{PF}}{k_B T}\right), \quad (2)$$

where $\beta_{PF} = (e^3/\pi\varepsilon_0\varepsilon_r)^{1/2}$ is the Poole–Frenkel coefficient, $\varepsilon_r$ is the dielectric constant in the optical frequency range, $\Phi_{PF}$ is the trap level, $k_B$ is the Boltzmann's constant, $T$ is absolute temperature, and $\sigma_0$ is a constant. The slope in Fig. 3(b) is about 10.87, which is consistent with the calculated slope 11.69. Here we choose the dielectric constant 6.30 in the optical frequency range (fricative index $n = 2.51$ at $\lambda = 500$ nm) for BTO films [20].

At forward bias (>0.1 V), Fig. 3(d) shows that the *I–V* curve can be fitted by SCLC mechanism since the slopes are mostly close to 2. Bayhan et al. indicated that the merging and leveling of log *I–V* curves may be due to SCLC conduction mechanism [21], which can also be seen from the *I–V* curves at forward bias in Fig. 2.

The C–V curves in Fig. 4 reveal a hysteretic and asymmetric behavior. The hysteretic behavior comes from the ferroelectric nature of BTO thin film. It is worth to note that the corresponding voltage value of short dash line is about −0.56 V, not zero. The C–V measurements indicate that a positive internal electric field was established in Pt/BTO/NSTO structure, which directs toward the NSTO bottom electrode.

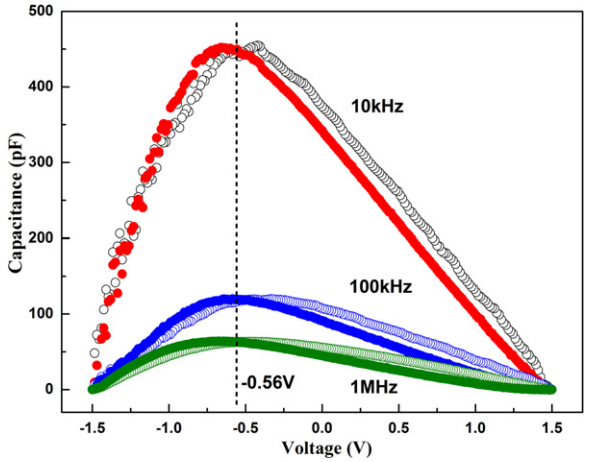


**Fig. 4.** C–V curves of the Pt/BTO/NSTO capacitor at different frequency. Open markers, voltage sweep up; solid markers, voltage sweep down.

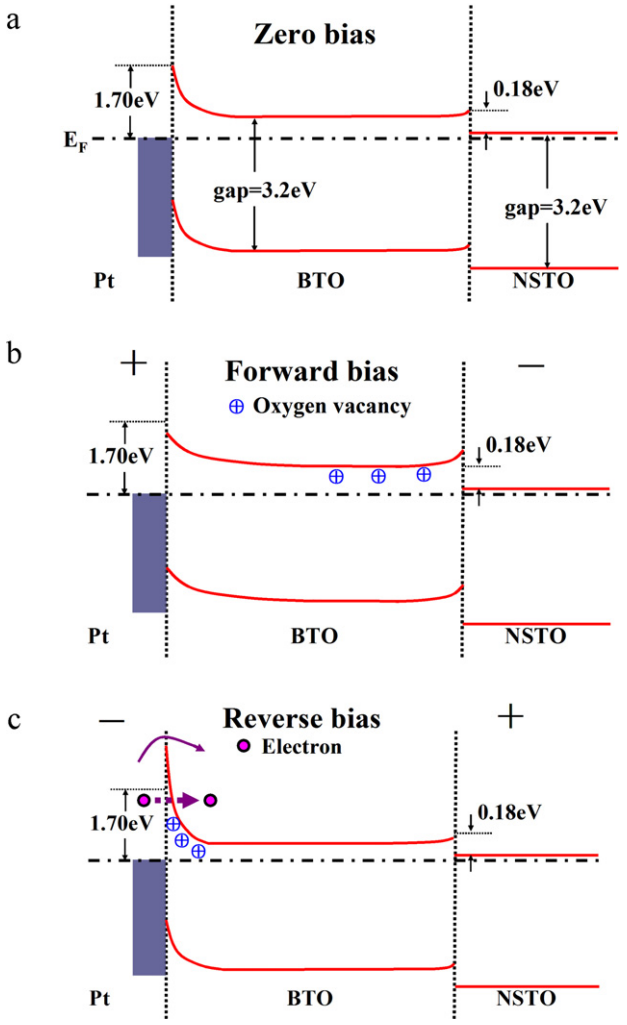


**Fig. 5.** Schematic band diagrams of the Pt/BTO/NSTO structure under different biasing conditions: (a) zero bias, (b) forward bias and (c) reverse bias.

The backward rectifying behavior can be explained by the modulation of the interface barrier width driven by the migration of oxygen vacancies. The Schottky-like barrier model considering the migration of oxygen vacancies driven under electric fields, which was reported by Sawa et al. [22,23], might be responsible for the rectifying behavior. When a forward bias is added, oxygen vacancies migrate away from the interface of Pt/BTO and move toward the interface of BTO/NSTO, which cause the interface barrier wider. The electrons are blocked to inject into Pt electrode. So the current is small and space-charge-limited (see Fig. 5(b)). Under a reverse bias, oxygen vacancies with positive charges move to the Pt/BTO interface through the grain boundaries in the BTO film, which narrows the Schottky barrier [23–25]. This may result in the P–F emission and F–N tunneling of electrons into the conduction band of the BTO film (see Fig. 5(c)).

## 4. Conclusions

The $BaTiO_3$ thin film was prepared on the Nb-doped $SrTiO_3$ single crystal substrates using pulsed laser deposition technique. The Schottky barrier formed at the Pt/BTO interface. The current–voltage curves exhibit backward diode-like rectifying character at reverse bias. About two orders of the rectification ration are achieved at reverse bias 4 V. The accumulation of the oxygen vacancies results in lowering and narrowing of the Schottky barrier near the interface region of Pt/BTO, which caused leakage current increase sharply as negative bias was added. At forward bias, the current were fitted by the space-charge-limited current mechanism. At reverse bias, the leakage current mechanisms were dominated by the Poole–Frenkel emission and Fowler–Nordheim tunneling near the Pt/BTO interface at lower bias and higher bias, respectively. The C–V measurements confirm such backward rectifying behavior.

## Acknowledgements

This work has been supported by the National Natural Science Foundation of China (no. 50972040), the Fund of international cooperation project of Wuhan City and Hubei Province (nos. 201070934339, 2010BFA010) and the Fund of Morning Program (no. 200950431161).

## References

[1] S. Liu, X.P. Liu, Y.S. Chen, R.Y. Jiang, J. Alloys Compd. 506 (2010) 877.
[2] A.S. Kavasoglu, O. Birgi, N. Kavasoglu, G. Oylumluoglu, A.O. Kodolbas, R. Kangi, O. Yilmaz, J. Alloys Compd. 509 (2011) 9394.
[3] H. Yang, H.M. Luo, H. Wang, I.O. Usov, N.A. Suvorova, M. Jain, D.M. Feldmann, P.C. Dowden, R.F.D. Paula, Q.X. Jia, Appl. Phys. Lett. 92 (2008) 102113.
[4] A. Gruverman, D. Wu, H. Lu, Y. Wang, H.W. Jang, C.M. Folkman, M.Y. Zhuravlev, D. Felker, M. Rzchowski, C.B. Eom, E.Y. Tsymbal, Nano Lett. 9 (2009) 3539.
[5] X.H. Wei, W. Huang, Z.B. Yang, J.H. Hao, Scripta Mater. 65 (2011) 323.
[6] Y.M. Cui, L.W. Zhang, C.C. Wang, G.L. Xie, Appl. Phys. Lett. 86 (2005) 203501.
[7] Y.M. Cui, L.W. Zhang, R.M. Wang, G.L. Xie, Thin Solid Films 516 (2008) 2292.
[8] Y.T. Zhang, C.C. Wang, X.M. Feng, M. He, H.B. Lu, Solid State Commun. 149 (2009) 2065.
[9] Z. Luo, P.K.L. Chan, K.L. Jim, C.W. Leung, Physica B 406 (2011) 3104.
[10] W.F. Liu, S.Y. Wang, C. Wang, Physica B 406 (2011) 3406.
[11] G.Y. Gao, Y. Wang, Y. Jiang, L.F. Fei, N.Y. Chan, H.L.W. Chan, W.B. Wu, Thin Solid Films 519 (2011) 6148.
[12] S.M. Sze, Physics of Semiconductor Devices, 3rd ed., Wiley, New York, 2007.
[13] V.M. Voora, T. Hofmann, M. Brandt, M. Lorenz, M. Grundmann, N. Ashkenov, M. Schubert, Appl. Phys. Lett. 94 (2009) 142904.
[14] T. Yoshimura, N. Fujimura, T. Ito, J. Cryst. Growth 174 (1997) 790.
[15] S.B. Mi, C.L. Jia, T. Heeg, O. Trithaveesak, J. Schubert, K. Urban, J. Cryst. Growth 283 (2005) 425.
[16] G.Y. Yang, S.I. Lee, Z.J. Liu, C.J. Anthony, E.C. Dickey, Z.K. Liu, C.A. Randall, Acta Mater. 54 (2006) 3513.
[17] H. Yang, M. Jain, N.A. Suvorova, H. Zhou, H.M. Luo, D.M. Feldmann, P.C. Dowden, R.F. DePaula, S.R. Foltyn, Q.X. Jia, Appl. Phys. Lett. 91 (2007) 072911.
[18] H.Y. Peng, G.P. Li, J.Y. Ye, Z.P. Wei, Z. Zhang, D.D. Wang, G.Z. Xing, T. Wu, Appl. Phys. Lett. 96 (2010) 192113.
[19] M.M. Hejazi, A. Safari, J. Appl. Phys. 110 (2011) 103710, And the references cited therein.
[20] M. Wöhlecke, V. Marrello, A. Onton, J. Appl. Phys. 48 (1977) 1748.
[21] H. Bayhan, S. Özden, Solid-State Electron. 50 (2006) 1563.
[22] C.J. Won, Y.A. Park, K.D. Lee, H.Y. Ryu, N. Hur, J. Appl. Phys. 109 (2011) 084108.
[23] A. Sawa, T. Fujii, M. Kawasaki, Y. Tokura, Appl. Phys. Lett. 85 (2004) 4073.
[24] X.G. Guo, X.S. Chen, Y.L. Sun, L.Z. Sun, X.H. Zhou, Phys. Lett. A 317 (2003) 501.
[25] X.B. Yan, Y.D. Xia, H.N. Xu, X. Gao, H.T. Li, R. Li, J. Yin, Z.G. Liu, Appl. Phys. Lett. 97 (2010) 112101.